ACMSR Taiwan Branch 澳亞醫學科學研究學會 台灣分會

澳亞醫學科學研究學會台灣分會 電子報

第五期 (2016/07)

編輯/ 張瑞芝理事 、鄭文玲秘書

校稿/ 劉青山秘書長

秘書長劉青山醫師的分享

不久前參加中華民國人類遺傳學會 2016 春季研討會，主要針對全國新生兒篩檢，尤其是以黏多醣症以及溶解體 POMPE 疾病之全國統計報告，同時針對黏多醣各種分型之酵素療法適應症作簡介，會員對於各樣適應症之規定皆有所疑慮及操作型定義，因爲此兩種疾病之酵素篩檢，以及酵素治療皆是造成國家的罕病治療經費大幅增加，尤其是 POMPE 心臟型變異之診斷及治療，與會之會員皆有不同之看法，甚至病友代表加入討論。會中也有請前國健局局長、現任奇美醫院遺傳中心主任林秀娟教授演講，演講中特別提出國家如何評估罕見疾病之合理醫療費用分布，尤其目前血友病及其他罕見疾病之新治療藥物問世，然而這些藥物之價格近乎天價，但是每個罕見疾病都是一條生命，如何在台灣健保醫療財務不足，又必須顧其各種病人之權利，甚至目前癌症標靶治療藥物，心血管特殊治療技術出現，勢必未來合理之國內醫療分配問題，將逐漸浮出，本次會議主要探討合理之酵素補充治療條件，也讓會員有充分表達各醫學中心治療上之瓶頸，以及申請藥物補助流程之公平性。

此次的訓練活動值得我們學習之處:

1. 台灣人類遺傳學會辦理了很重要之罕病健保資源分配專家座談會，此專家座談會可以提供未來健保罕病治療財源分配之公平性。

2. 各樣罕病治療必須確認診斷之正確性，因不同基因型之同一類疾病，如黏多醣及 POMPE 皆有可能對酵素治療反應不同，並且需要有良好之病患醫界溝通平台，例如舉辦公聽會，否則未來罕病新藥會每年逐增，進而造成健保財務赤字。

3. 醫學倫理必須介入到罕病酵素替代治療，畢竟台灣還有其他疾病須做緊急治療，況且罕病治療之費用是終身性的，國家爲一個罕病患者一年花費從 100 萬至 1000 萬，醫學倫理必須思考生命無價，但又必須兼顧健保資源財務分配之公平及正義，未來國家醫療政策必須特別注重此種健保資源分配主題。

4. 國內必須要建構一致性技術之基因檢測及酵素檢測，並且台灣人有與國外之不同基因型發現，因此我們國內必須有公認並且接受外部認證之中央實驗室，擴展診斷精確度。

5. 罕病研究及關懷團隊可加入中華民國人類遺傳學會，學習各樣重要之遺傳疾病診斷治療以及全人關懷，也可將相關訊息傳遞到彰基澳亞醫學科學研究學會台灣分會，促成在此議題之學習以及病人關懷上。

研究成果

恭喜血管暨基因體研究中心張瑞芝研究員論文獲得 Translational Research 期刊發表 Transl Res. 2016 Apr;170:40-56.e3

Allogeneic/xenogeneic transplantation of peptide-labeled mitochondria in Parkinson's disease: restoration of mitochondria functions and attenuation of 6-hydroxydopamine-induced neurotoxicity.

Chang JC, Wu SL, Liu KH, Chen YH, Chuang CS, Cheng FC, Su HL, Wei YH, Kuo SJ, Liu CS.

Abstract

Although restoration of mitochondrial function in mitochondrial diseases through peptide-mediated allogeneic mitochondrial delivery (PMD) has been demonstrated in vitro, the in vivo therapeutic efficacy of PMD in Parkinson's disease (PD) has yet to be determined. In this study, we compared the functionality of mitochondrial transfer with or without Pep-1 conjugation in neurotoxin (6-hydroxydopamine, 6-OHDA)-induced PC12 cells and PD rat models. We injected mitochondria into the medial forebrain bundle (MFB) of the PD rats after subjecting the nigrostriatal pathway to a unilateral 6-OHDA lesion for 21 days, and we verified the effectiveness of the mitochondrial graft in enhancing mitochondrial function in the soma of the substantia nigra (SN) neuron through mitochondrial transport dynamics in the nigrostriatal circuit. The result demonstrated that only PMD with allogeneic and xenogeneic sources significantly sustained mitochondrial function to resist the neurotoxin-induced oxidative stress and apoptotic death in the rat PC12 cells. The remaining cells exhibited a greater capability of neurite outgrowth. Furthermore, allogeneic and xenogeneic transplantation of peptide-labeled mitochondria after 3 months improved the locomotive activity in the PD rats. This increase was accompanied by a marked decrease in dopaminergic neuron loss in the substantia nigra pars compacta (SNc) and consistent enhancement of tyrosine hydroxylase-positive immunoreaction of dopaminergic neurons in the SNc and striatum. We also observed that in the SN dopaminergic neuron in the treated PD rats, mitochondrial complex I protein and mitochondrial dynamics were restored, thus ameliorating the oxidative DNA damage. Moreover, we determined signal translocation of graft allogeneic mitochondria from the MFB to the calbindin-positive SN neuron, which demonstrated the regulatory role of mitochondrial transport in alleviating 6-OHDA-induced degeneration of dopaminergic neurons.

最新消息

• • •

「2016 彰基第 10 屆國際基因體醫學研討會＆第 4 屆澳亞醫學科學研究研討會＆2016 台灣粒線體醫學暨研究學會學術研討會暨年會」將於 2016 年 09 月 24-25 日於彰基舉辦。歡迎各位會員踴躍參加並轉傳相關訊息。詳情請參閱 http://www2.cch.org.tw/10thisgm_tw/

公開徵求『第二屆澳亞醫學科學研究學會台灣分會 理、監事候選人』，日前，若無人自薦將由理事長推派候選人於 09 月 24 日會員大會時，進行理監事改選。

如對本中心或發行之電子報 有任何疑問，或欲分享您專業領域之科學新知。歡迎 Email 至 acmsrtaiwan@gmail.com.

Nature. 2016 Apr 7;532(7597):112-6. doi: 10.1038/nature17399. Epub 2016 Mar 30.

Mitochondrial ROS regulate thermogenic energy expenditure and sulfenylation of UCP1.

Chouchani ET[1,2], Kazak L[1,2], Jedrychowski MP[2], Lu GZ[1,2], Erickson BK[2], Szpyt J[2], Pierce KA[3], Laznik-Bogoslavski D[1], Vetrivelan R[4], Clish CB[3], Robinson AJ[5], Gygi SP[2], Spiegelman BM[1,2].

Author information

[1]Dana-Farber Cancer Institute, Harvard Medical School, Boston, Massachusetts 02115, USA.

[2]Department of Cell Biology, Harvard Medical School, Boston, Massachusetts 02115, USA.

[3]Broad Institute of Harvard and MIT, Cambridge, Massachusetts 02142, USA.

[4]Department of Neurology, Harvard Medical School, Boston, Massachusetts 02215, USA.

[5]MRC Mitochondrial Biology Unit, Hills Road, Cambridge CB2 0XY, UK.

Abstract

Brown and beige adipose tissues can dissipate chemical energy as heat through thermogenic respiration, which requires uncoupling protein 1 (UCP1). Thermogenesis from these adipocytes can combat obesity and diabetes, encouraging investigation of factors that control UCP1-dependent respiration in vivo. Here we show that acutely activated thermogenesis in brown adipose tissue is defined by a substantial increase in levels of mitochondrial reactive oxygen species (ROS). Remarkably, this process supports in vivo thermogenesis, as pharmacological depletion of mitochondrial ROS results in hypothermia upon cold exposure, and inhibits UCP1-dependent increases in whole-body energy expenditure. We further establish that thermogenic ROS alter the redox status of cysteine thiols in brown adipose tissue to drive increased respiration, and that Cys253 of UCP1 is a key target. UCP1 Cys253 is sulfenylated during thermogenesis, while mutation of this site desensitizes the purine-nucleotide-inhibited state of the carrier to adrenergic activation and uncoupling. These studies identify mitochondrial ROS induction in brown adipose tissue as a mechanism that supports UCP1-dependent thermogenesis and whole-body energy expenditure, which opens the way to improved therapeutic strategies for combating metabolic disorders.

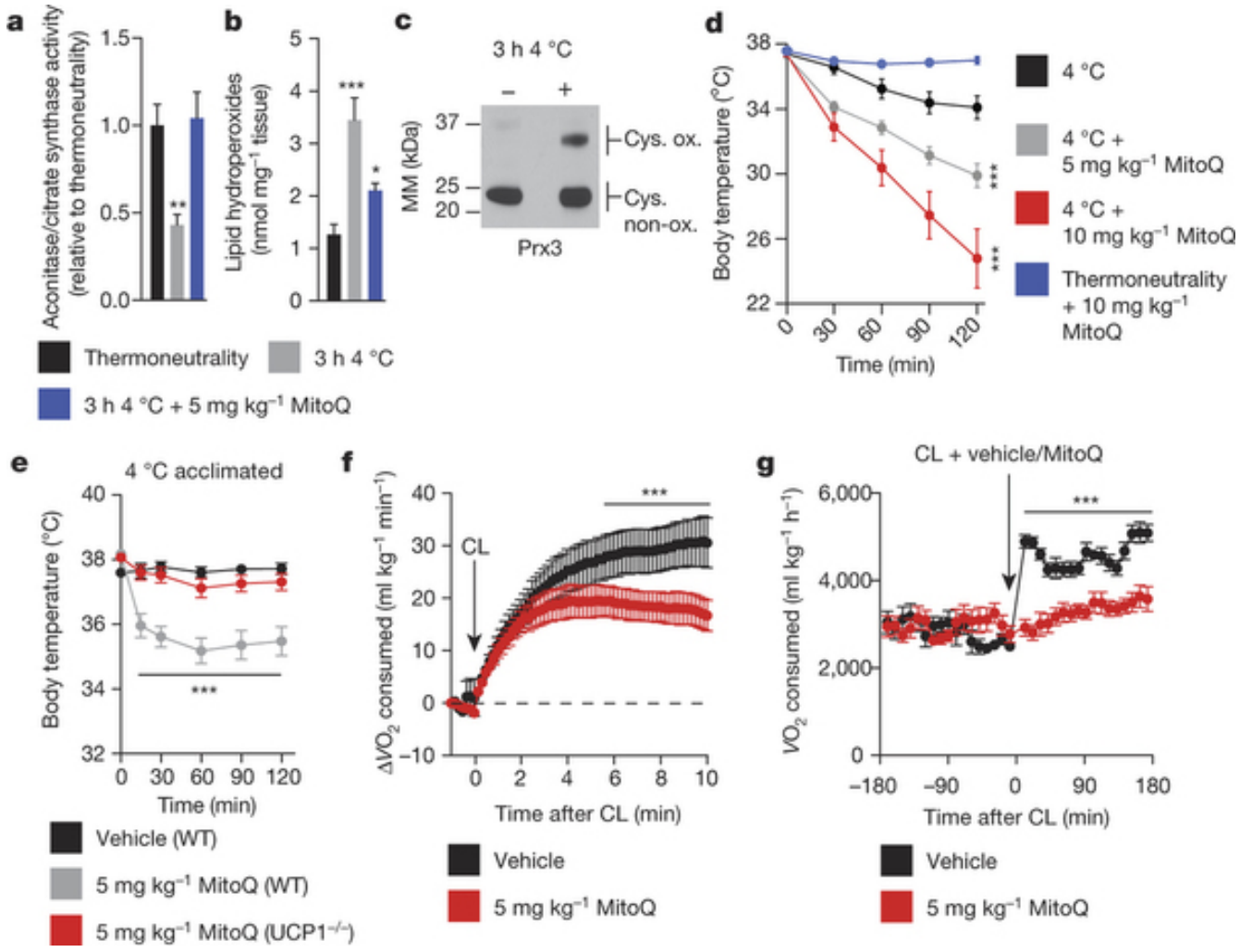

Figure 1:Increased BAT mitochondrial ROS levels support UCP1-dependent thermogenesis *in vivo*.

a–**c**, Effect of acute cold exposure on in vivo BAT (**a**) mitochondrial superoxide-dependent inactivation of mitochondrial aconitase (n = 5; 5 mg kg^{-1} MitoQ n = 4), (**b**) lipid hydroperoxide content (n = 5), and (**c**) mitochondrial hydrogen-peroxide-dependent oxidation of Prx3. Oxidized Prx3 was assessed using the redox gel shift method described in Methods. MM, molecular mass. Cys. ox., cysteine oxidation. For uncropped scans see **Supplementary Figs 1–3**. **d**, Effect of i.p. MitoQ on core body temperature after acute cold exposure (n = 10). **e**, Effect of i.p. MitoQ on core body temperature of WT and $UCP1^{-/-}$ mice after 4 °C acclimation (n = 10; $UCP1^{-/-}$ n = 8). **f**, Oxygen consumed acutely before and after i.p. CL ± MitoQ (n = 5). **g**, Oxygen consumed 3 h before and after i.p. CL ± MitoQ (n = 8). Data are mean ± s.e.m. of at least four mouse replicates. *P < 0.05, ***P < 0.001 (two-tailed Student's t-test for pairwise comparisons, one-way/two-way analysis of variance (ANOVA) for multiple comparisons involving one/two independent variables).

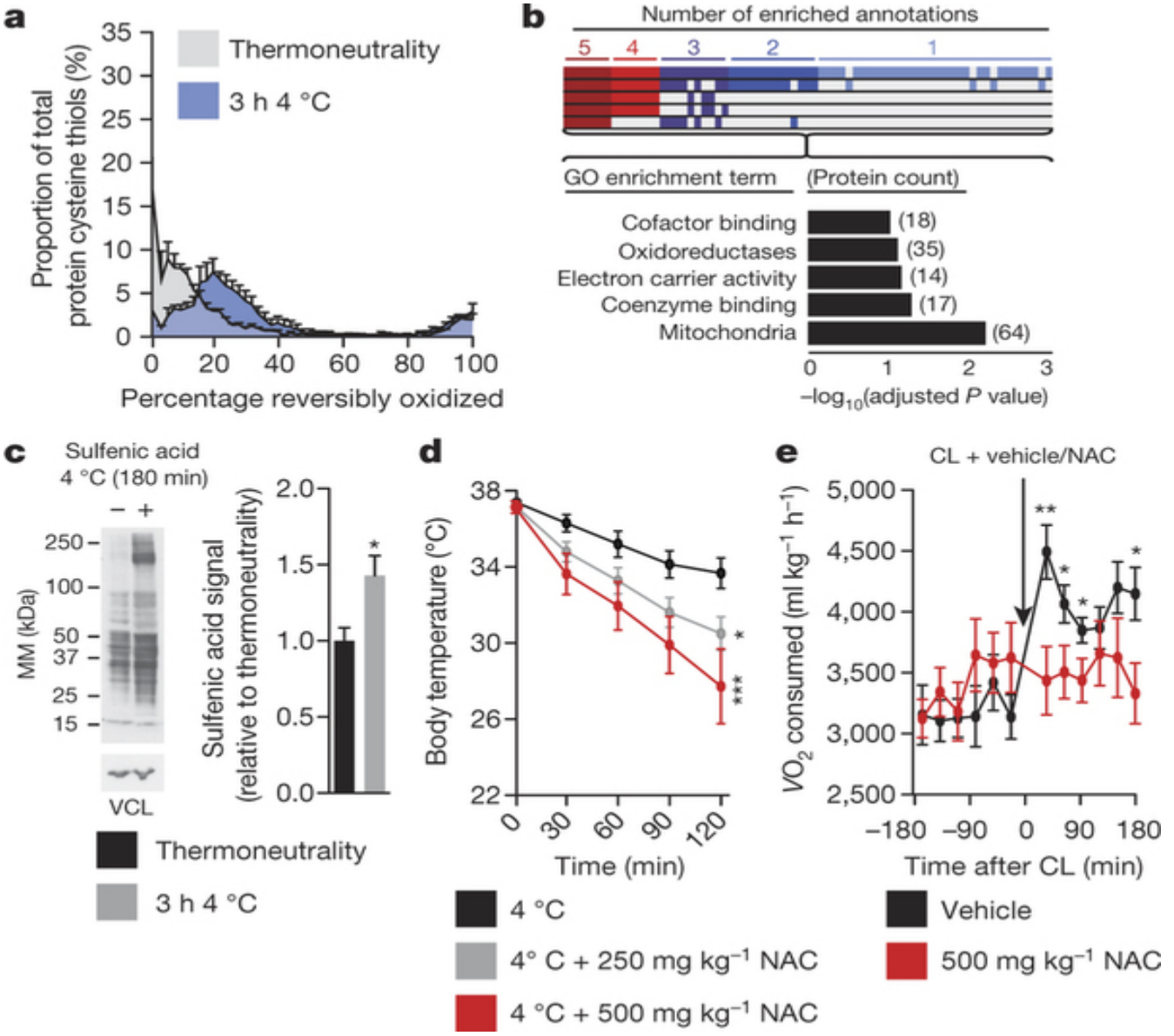

Figure 2: BAT mitochondrial ROS during thermogenesis drives oxidation of cellular and mitochondrial thiols.

a, Distribution of percentage reversible oxidation status of BAT protein thiols ± acute cold exposure. **b**, Pathway analysis of BAT proteins containing cysteine residues sensitive to substantial oxidation (>10% shift in oxidation status) upon cold exposure. Top: proteins clustered according to shared GO enrichment terms. Bottom: significantly enriched pathways. **c**, Immunodetection of protein sulfenic acid levels in BAT ± acute cold exposure (n = 4) **d**, Effect of i.p. NAC on core body temperature after acute cold exposure (n = 8; 500 mg kg^{-1} NAC n = 7). **e**, Oxygen consumed 3 h before and after i.p. CL ± NAC (control n = 12; NAC n = 9). VCL, vinculin. Data are mean ± s.e.m. of at least four mouse replicates. *P < 0.05, **P < 0.01, ***P < 0.001 (two-tailed Student's t-test for pairwise comparisons, one-way/two-way ANOVA for multiple comparisons involving one/two independent variables).

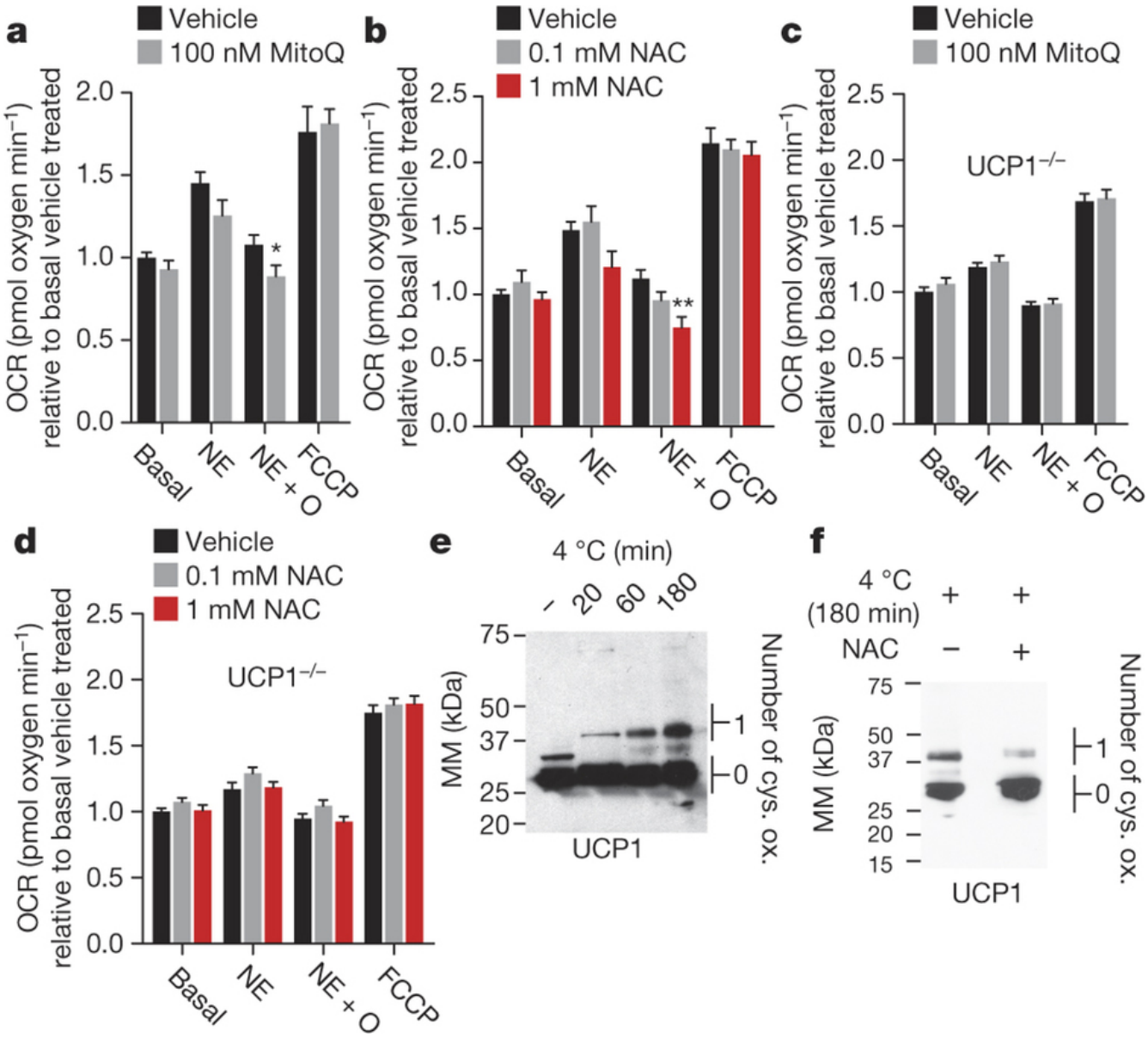

Figure 3: BAT mitochondrial ROS oxidatively modify a cysteine residue on UCP1 and support UCP1-dependent leak respiration.

a, ***b***, *OCR of brown adipocytes ± noradrenaline (NE) stimulation + oligomycin to determine leak respiration ± (**a**) MitoQ (*n *= 10) or (**b**) NAC (*n *= 8; 0.1 mM NAC* n *= 7).* ***c***, ***d***, *OCR of primary UCP1$^{-/-}$ adipocytes ± noradrenaline stimulation + oligomycin ± (**c**) MitoQ (*n *= 10) or (**d**) NAC (*n *= 10).* ***e***, ***f***, *Cys-redox immunoblot of BAT UCP1 (**e**) after a time course of acute cold exposure, and (**f**) after acute cold exposure ± 500 mg kg^{-1} NAC. FCCP, carbonyl cyanide-*p*-trifluoromethoxyphenylhydrazone. Data are mean ± s.e.m. of at least seven cellular replicates. *P < 0.05, **P < 0.01 (two-tailed Student's* t*-test for pairwise comparisons, one-way ANOVA for multiple comparisons).*

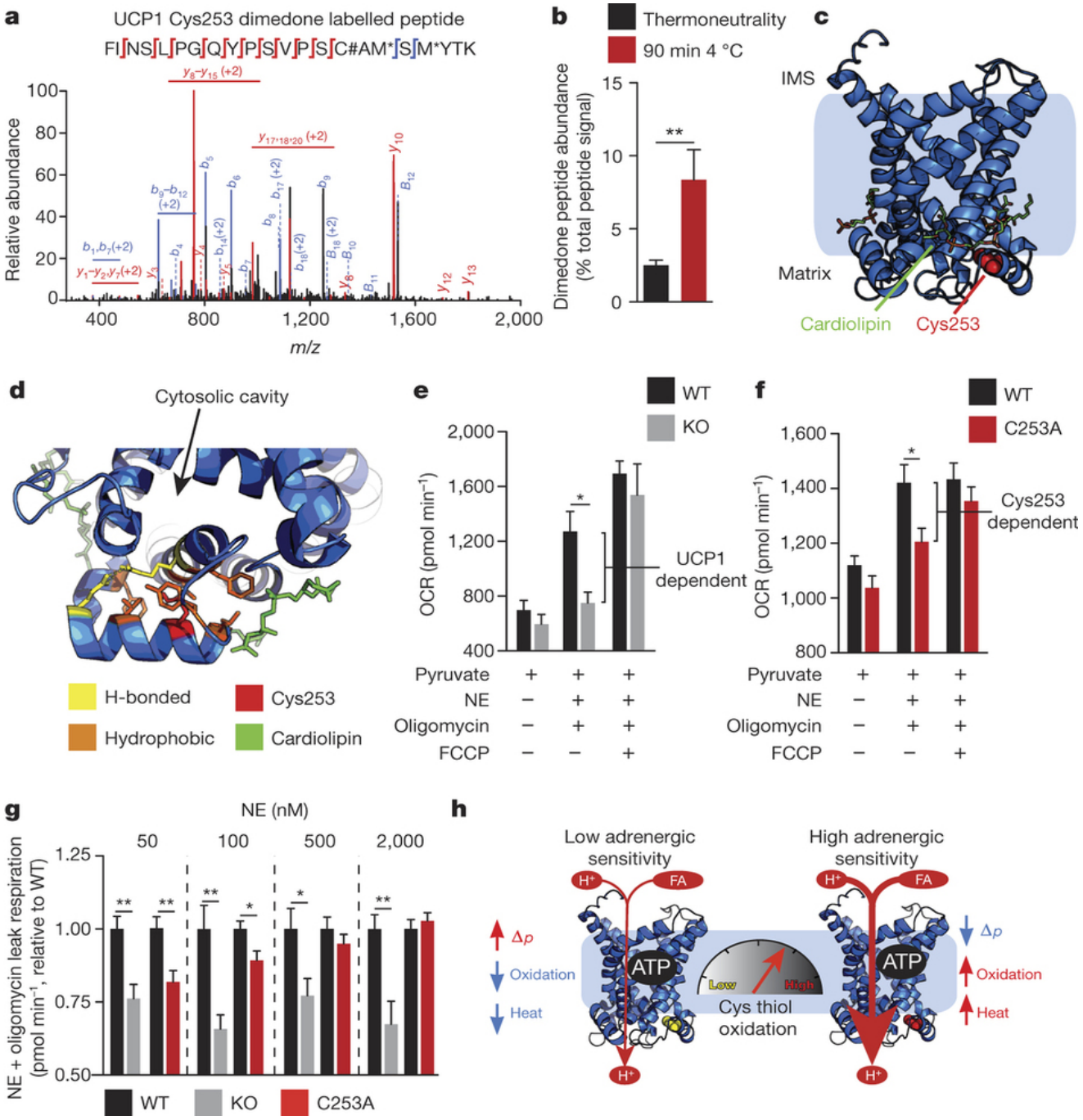

Figure 4: UCP1 Cys253 is sulfenylated during thermogenesis and sensitizes UCP1 to adrenergic activation.

a, MS^2 spectrum of dimedone-labelled UCP1 Cys253 peptide indicating sulfenylation of this site during thermogenesis. Fragment ions that span the dimedone-alkylated cysteine are highlighted in the peptide sequence. C#, dimedone-labelled cysteine; M*, oxidized methionine. **b**, Quantification of dimedone-labelled UCP1 Cys253 relative to the NEM-alkylated form (n = 5). **c**, **d**, Structure of (**c**) human UCP1 modelled on the AAC crystal structure and (**d**) Cys253 in a hydrophobic pocket between two matrix facing helices. IMS, intermembrane space. **e**, **f**, Basal, maximal, and UCP1-dependent OCR of UCP1$^{-/-}$ brown adipocytes ± transduction with (**e**) WT UCP1 (WT n = 7; UCP1$^{-/-}$ n = 6) or (**f**) UCP1 C253A (WT n = 17; C253A n = 19). KO, knockout. **g**, UCP1-dependent leak respiration after stimulation by various concentrations of noradrenaline (50 nM noradrenaline n = 9; 100 nM noradrenaline n = 7; 500 nM noradrenaline n = 8; 2,000 nM noradrenaline n = 6). Comparison of UCP1 WT and C253A indicates that degree of UCP1 inhibition by C253A is inversely correlated with noradrenaline concentration (n = 19; 100 nM WT noradrenaline; n = 17,500 nM noradrenaline n = 18; 2,000 nM noradrenaline n = 10). **j**, A model of sensitization of UCP1-mediated uncoupling by mitochondrial ROS. Data are mean ± s.e.m. of at least five mouse replicates or cell replicates for respirometry experiments. *P < 0.05, **P < 0.01 (two-tailed Student's t-test for pairwise comparisons).

Int J Biol Sci. 2016 Feb 29;12(5):532-44. doi: 10.7150/ijbs.15153. eCollection 2016.

Mitochondrial Stat3, the Need for Design Thinking

Rui Yang, Mercedes Rincon

Author information

Department of Medicine/Immunobiology Program, University of Vermont, Burlington, VT, USA, 05405
Corresponding author: University of Vermont College of Medicine, Given Medical Building Room C331, 89 Beaumont Ave., Burlington, VT 05405-0068, USA.Phone: 802-656-0937; email: mrincon@uvm.edu

Abstract

Stat3 has been studied extensively as a transcription factor, however the finding that Stat3 also localizes to mitochondria has opened a new area to discover non-classical functions. Here we review the current knowledge of mitochondrial Stat3 as a regulator of the electron transport chain (ETC) and its impact on mitochondrial production of ATP and ROS. We also describe recent findings identifying Stat3 as a regulator of mitochondrial Ca2+ homeostasis through its effect on the ETC. It is becoming evident that these non-classical functions of Stat3 can have a major impact on cancer progression, cardiovascular diseases, and inflammatory diseases. Therefore, mitochondrial Stat3 functions challenge the current design of therapies that solely target Stat3 as a transcription factor and suggest the need for "design thinking," which leads to the development of novel strategies, to intervene the Stat3 pathway.

Keywords: Stat3

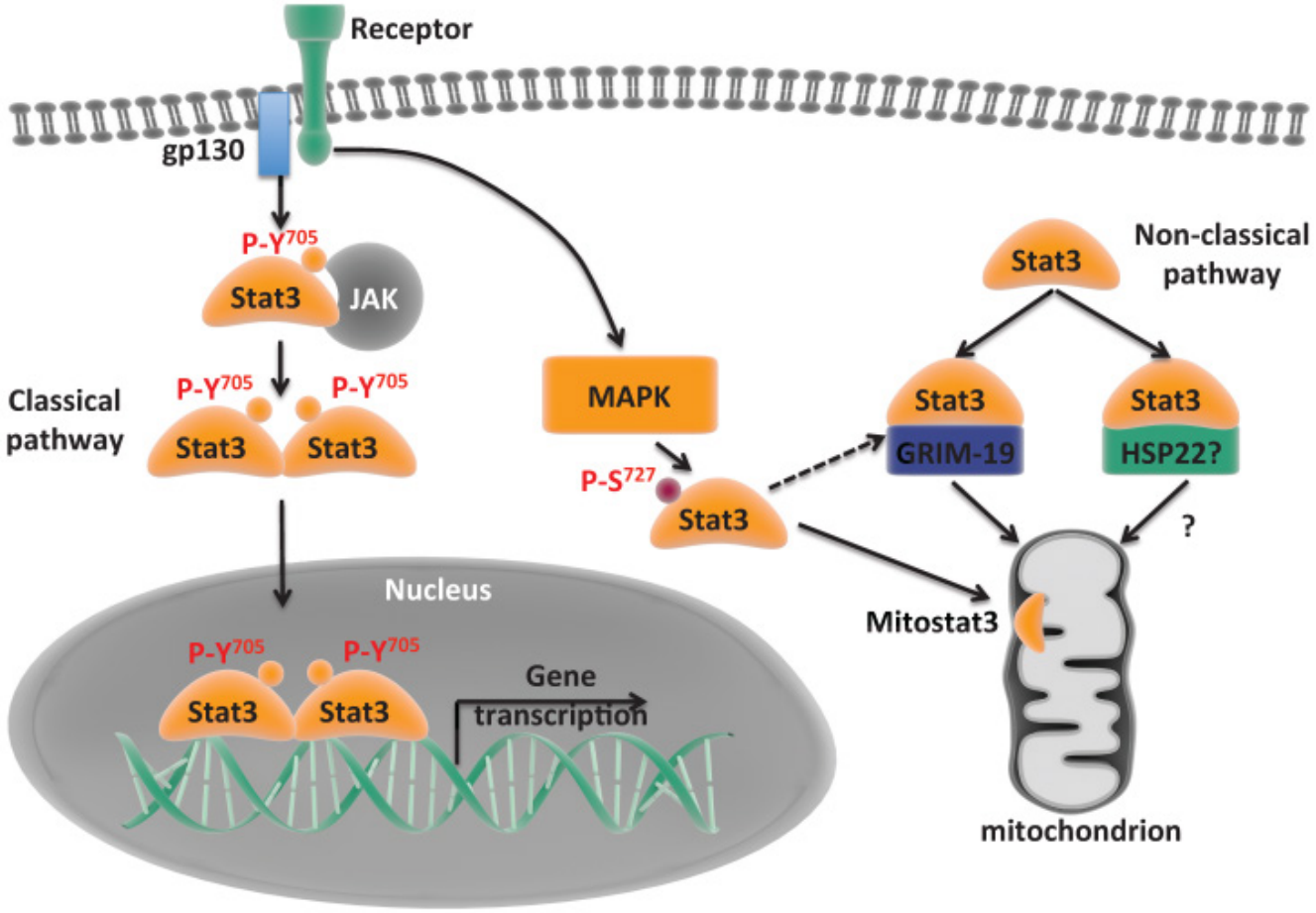

Figure 1. Classical and non-classical pathways of Stat3. Classical pathway where Stat3 translocates to the nucleus and mediates gene transcription.Non-classical pathway where Stat3 is recruited to mitochondria and regulates functions alternative to transcription.

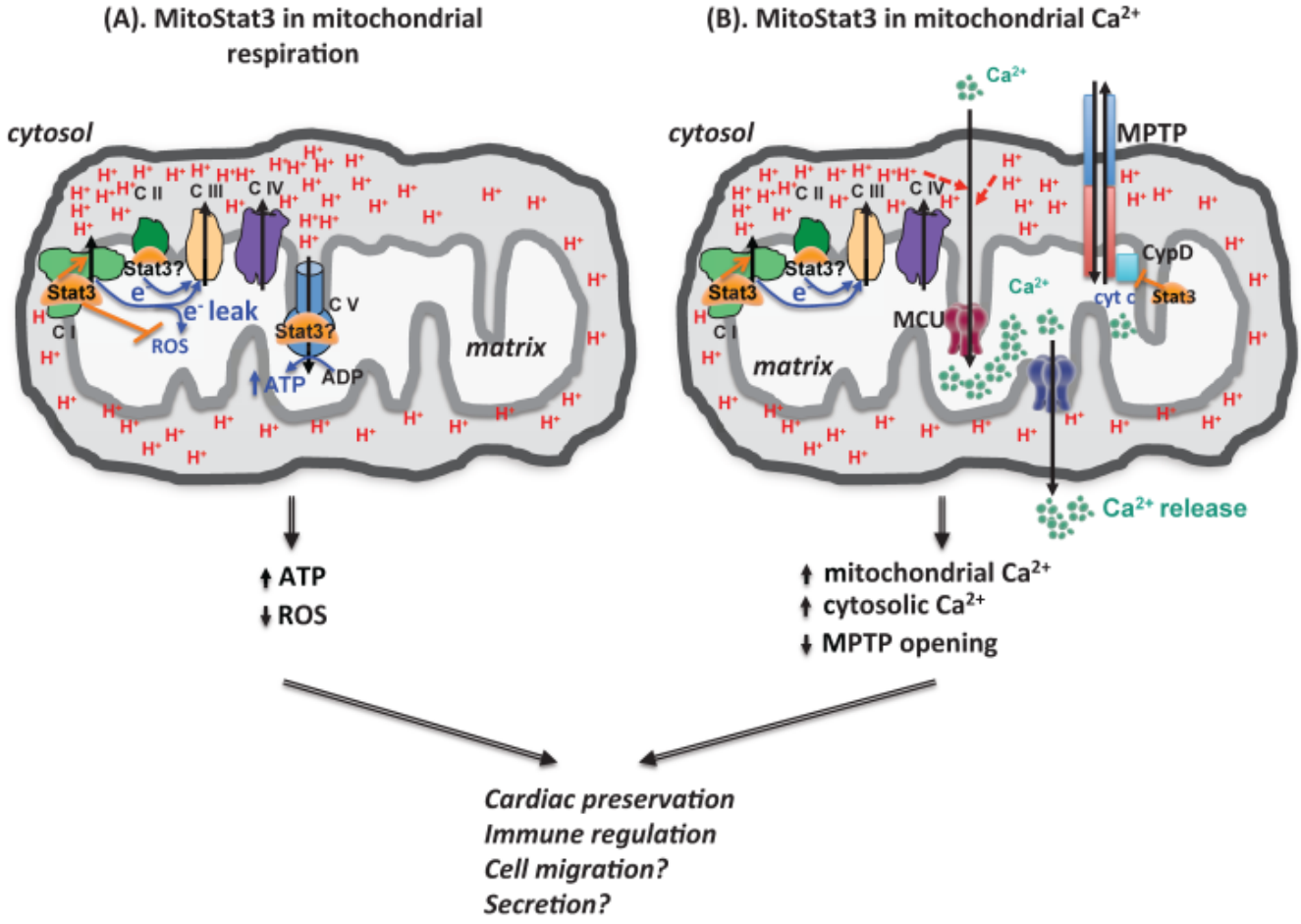

Figure 2.mitoStat3 as a regulator of mitochondria functions.(A) mitoStat3 promotes mitochondrial respiration (ATP synthesis) by increasing ETC activity and MMP. ***(B)*** mitoStat3 regulates mitochondrial Ca2+ and cytosolic Ca2+ through the regulation of ETC and MPTP.

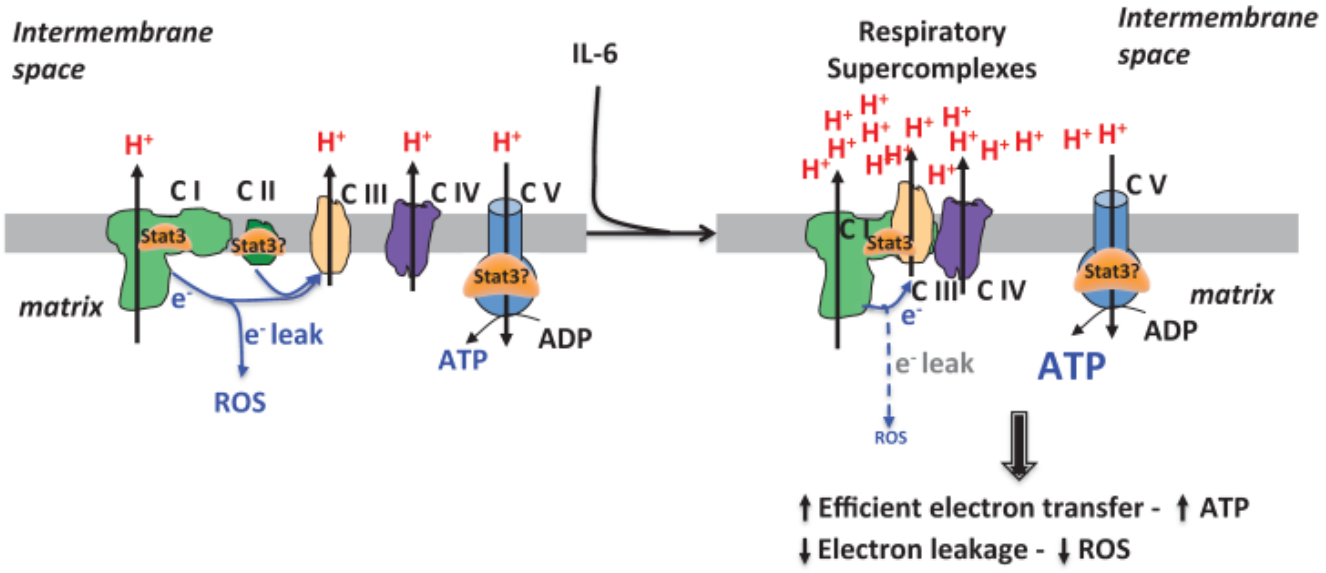

Figure 3.mitoStat3 as a regulator of respiratory supercomplexes. Stat3 can be recruited to respiratory supercomplexes to promote ETC activity and ATPsynthesis without increasing ROS production.

Table 1. Promising anti-tumor Stat3 inhibitors that target mitochondrial functions

Inhibitor	Target Site	Function	Mitochondrial Effects
AG490	JAK2 kinases, Stat3 tyr phosphorylation [138, 139]	↑ malignant cells apoptosis, ↓ malignant cell growth, ↓ malignant cell invasion [140-143]	↓ mitochondrial membrane potential in astrocytes [43] ↑ ROS production in astrocytes [43] ↓ cardioprotective preservation of mitochondrial function by inhibition of mitoStat3 in myocardial I/R injury [28] ↑ MPTP opening [149, 150] ↓ neuroprotective effects by leptin-mediated mitochondrial stabilization [144] ↓ cardioprotective effects by melatonin-mediated mitochondrial preservation in myocardial I/R injury [151] ↓ cardioprotective effects by the reduced MPTP opening elicited by leptin and atorvastatin in myocardial I/R injury [149, 150]
Stattic	Stat3 phosphorylation, SH2 domain [71]	↑ malignant cells apoptosis, ↓ malignant cell growth, ↑ tumor chemo- and radiosensitivity [123-125]	↓ mitochondrial ADP-stimulated oxygen consumption in cardiomyocytes [30] ↓ ATP production in human sperms and mast cells [24, 112] ↓ oxygen consumption rates and ↓ ETC complex II and complex III activities in mast cells [112] ↓ mitochondrial membrane potential in human sperms [24] ↑ ROS production in human sperms [24] ↓ cardioprotective preservation of mitochondrial function by mitoStat3 activation in myocardial I/R injury [28] ↑ ROS production in cardiomyocytes, and subsequent ↑ MPTP opening and ↓ ATP production [71] ↑ cellular injuries due to ↑ MPTP opening by mitoStat3 inhibition in myocardial I/R injury [30] ↓ mast cell degranulation through the inhibition of mitochondrial function [112]
Cucurbitacin-I/JSI-124	Stat3 tyr phosphorylation [130]	↑ malignant cells apoptosis, ↓ malignant cell growth [130-136]	↓ mitochondrial membrane potential [137] ↑ ROS production and subsequent ↑ autophagy [136] ↑ mitochondrial apoptotic cell death in cancer cells [131-133]
MDC-1112/phospho-valproic acid	Stat3 phosphorylation, mitochondrial Stat3 accumulation [129]	↑ malignant cells apoptosis, ↓ malignant cell growth [129]	↓ mitoStat3 mitochondrial accumulation [129] ↓ mitochondrial membrane potential [129] ↑ mitochondrial apoptotic cell death [129]
FLLL32	Stat3 tyr phosphorylation [127, 128]	↑ malignant cells apoptosis [127, 128]	↓ mitochondrial membrane potential [127] ↑ mitochondrial apoptotic cell death in cancer cells [127, 128]